Published in final edited form as:
Dev Biol. 2009 April 15; 328(2): 273–284. doi:10.1016/j.ydbio.2009.01.026.

EARLY ONSET OF CRANIOSYNOSTOSIS IN AN APERT MOUSE MODEL REVEALS CRITICAL FEATURES OF THIS PATHOLOGY

Greg Holmes, **Gerson Rothschild***, **Upal Basu Roy**, **Chu-Xia Deng****, **Alka Mansukhani**, and **Claudio Basilico**[1]
Department of Microbiology, New York University School of Medicine, New York, NY 10016, USA

Abstract

Activating mutations of FGFRs1–3 cause craniosynostosis (CS), the premature fusion of cranial bones, in man and mouse. The mechanisms by which such mutations lead to CS have been variously ascribed to increased osteoblast proliferation, differentiation, and apoptosis, but it is not always clear how these disturbances relate to the process of suture fusion. We have reassessed coronal suture fusion in an Apert Fgfr2 (S252W) mouse model. We find that the critical event of CS is the early loss of basal sutural mesenchyme as the osteogenic fronts, expressing activated Fgfr2, unite to form a contiguous skeletogenic membrane. A mild increase in osteoprogenitor proliferation precedes but does not accompany this event, and apoptosis is insignificant. On the other hand, the more apical coronal suture initially forms appropriately but then undergoes fusion, albeit at a slower rate, accompanied by a significant decrease in osteoprogenitor proliferation, and increased osteoblast maturation. Apoptosis now accompanies fusion, but is restricted to bone fronts in contact with one another. We correlated these *in vivo* observations with the intrinsic effects of the activated Fgfr2 S252W mutation in primary osteoblasts in culture, which show an increased capacity for both proliferation and differentiation. Our studies suggest that the major determinant of Fgfr2-induced craniosynostosis is the failure to respond to signals that would halt the recruitment or the advancement of osteoprogenitor cells at the sites where sutures should normally form.

Keywords

Fgfr2; craniosynostosis; Apert syndrome; osteoblast; coronal suture; calvaria; mouse; intramembranous ossification

INTRODUCTION

Activating mutations in FGFRs1–3 are the basis of many human bone morphogenetic disorders, as they affect the proliferation and differentiation of both chondrocytes and osteoblasts, the two major cell types involved in skeletal development. The shortened long bones and chondrodysplasias observed in humans and mice with activating FGFR3 mutations

1Corresponding Author: Department Of Microbiology, New York University School Of Medicine, New York, NY 10016. Phone: (212) 263-5341. Fax: (212) 263-8714. E-mail: E-mail: claudio.basilico@med.nyu.edu.
*Current Address: Department of Developmental and Regenerative Biology, Mt. Sinai Medical Center, Annenberg 25-98, 1 Gustave L. Levy Place, New York, NY 10029, USA
**Genetics Of Development And Disease Branch, National Institute Of Diabetes, Digestive And Kidney Diseases, US National Institutes Of Health, 10 Center Drive, Bethesda, Maryland 20892, USA

find a relatively simple explanation in the growth inhibitory and pro-apoptotic effects of FGF signaling in chondrocytes, where FGFR3 is highly expressed (Marie et al., 2005; Ornitz, 2005; Ornitz and Marie, 2002). However, the craniosynostosis syndromes produced by misregulated FGF signaling in osteoblasts currently defy a simple molecular explanation.

Craniosynostosis (CS) is the premature fusion of the flat bones of the skull. These bones form by intramembranous ossification, in which osteoblasts differentiate directly from osteogenic mesenchymal cells. Fibrous joints (sutures) between these bones act as growth sites to allow for skull growth to coordinate with and accommodate the growing brain, and the premature fusion of one or more of these sutures in CS adversely affects subsequent cranial and brain development (Opperman, 2000). The most commonly identified genetic lesions in syndromic CS are activating mutations in FGFRs1–3 and inactivating mutations of the transcription factor TWIST (Morriss-Kay and Wilkie, 2005). Apert syndrome is largely caused by activating mutations of Serine252 or Proline253 in FGFR2 (Wilkie et al., 1995). The affected residues lie in the linker region connecting the extracellular immunoglobulin-like domains II and III, affect both mesenchymal and epithelial splice forms of the receptor, and allow each to respond to a wider range of FGF ligands, increasing signaling (Yu et al., 2000). Premature fusion of the coronal suture is the primary skull defect of Apert syndrome (Cohen and Kreiborg, 1996).

The Serine252Tryptophan (S252W) mutation in mouse has been generated independently in two different laboratories (Chen et al., 2003; Wang et al., 2005). In the mouse, the coronal suture normally remains patent throughout life. The first Apert mouse model (Chen et al., 2003) demonstrated coronal suture fusion first signaled by an increased overlap of the frontal and parietal bones prenatally, followed by their progressive fusion from about postnatal (P) day 4. No differences in cell proliferation or differentiation of coronal suture osteoblasts was noted between wild-type (WT) and mutant mice, but an increase in the level of apoptosis in the mutant suture was proposed as the cause for suture fusion. In the second Apert mouse model midline sutures were affected differentially, while coronal and lambdoid suture fusion was noted, but otherwise not characterized (Wang et al., 2005).

The development of effective therapies for craniosynostosis requires an understanding of the process of suture fusion. Premature fusion of the cranial sutures in humans and mice with activating FGFR2 mutations has been varyingly ascribed to increased osteoblast proliferation, differentiation, or apoptosis (Chen et al., 2003; Eswarakumar et al., 2004; Marie et al., 2002). In culture, sustained FGF signaling stimulates osteoblast proliferation and inhibits their differentiation, while also increasing apoptosis when cells are exposed to differentiating conditions, but it is still not clear how these findings can be reconciled with the observations made *in vivo* (Mansukhani et al., 2000; Tang et al., 1996).

To identify the critical steps in osteoblast development that determine the cranial malformations caused by an activated Fgfr2, we have re-examined the mouse model of Apert syndrome described by Chen et al (2003), and tried to correlate the observations made *in vivo* in this animal model with the study of the properties of osteoblasts derived from the calvaria of the same mutant mice in culture. The results presented in this report show that suture fusion is a very early embryonic event in this Apert model, which is accompanied by an initial increase in cell proliferation followed by accelerated differentiation, as osteoblasts replace sutural mesenchyme. In mutant sutures, mature osteoblasts invade the sites where sutures should be formed and obliterate them. In culture, mutant osteoblasts also exhibit increased proliferation and ability to differentiate, and a variable downregulation of *Fgfr2* expression. Our results suggest that the major determinant of craniosynostosis induced by the Apert Fgfr2 mutation is the failure of the mutant suture mesenchyme to respond to the signals that would normally prevent the induction of the osteoblastic fate at the suture sites.

METHODS

Mice

Mice were initially bred from a founding pair (male *Fgfr2*$^{Neo\text{S252W/+}}$; female *EIIa-Cre*). They were also outbred to a Swiss-Webster background. Mice were genotyped by PCR of genomic DNA prepared from tail-tips or cultured cells for *Fgfr2*, *Neo*, and *Cre*. The primers for *Fgfr2* were as described (Chen et al., 2003). The sizes of the WT and *Cre*-excised mutant products were 393 bp and 457 bp, respectively, were confirmed by sequencing, and agree with published genomic sequence. These primers did not amplify the *Neo*-containing mutant allele under the PCR conditions used. The *Neo* primers were 5′-AGGATCTCCTGTCATCTCACCTTGCTCCTG-3′ and 5′-AAGAACTCGTCAAGAAGGCGATAGAAGGCG-3′ (492 bp). The *Cre* primers were 5′-CCTGGAAAATGCTTCTGTCCGTTTGCC-3′ and 5′-GAGTTGATAGCTGGCTGGTGGCAGATG-3′ (640 bp). *Cre* PCR was performed with 10% DMSO.

Histology and RNA *in situ* hybridization (ISH)

Embryos were fixed in 4% paraformaldehyde (PFA) in PBS at 4°C overnight, washed in PBS, equilibrated with 30% sucrose/PBS, then embedded in Tissue-Tek OTC Compound (Sakura, Japan). All PBS solutions were pre-treated with DEPC. Frozen sections of 10 μm thickness were cut on a Microm Cryostat and transferred to Superfrost/Plus microscope slides (Fisher Scientific, USA). Alkaline phosphatase (Alp) histochemistry was performed as described previously (Miao and Scutt, 2002), except that frozen sections were first dried at 37°C for 30 minutes, rehydrated in PBS for 5 minutes, and incubated with 0.1M Tris-maleate buffer, before detection with Fast Red TR/napthol AS-MX phosphate. For whole-mount detection of Alp at E12.5, fixed heads were stained with BM Purple AP Substrate (Roche). RNA *in situ* hybridization (ISH) was performed essentially as described (Xu and Wilkinson, 1999), except that older sections were treated with up to 75 ug/ml of Proteinase K for 10 minutes; RNase treatment was generally omitted. RNA riboprobes were prepared with DIG RNA Labeling Mix as described by the manufacturer (Roche). *Fgfr1* and *Fgfr2* clones were from G. Morriss-Kay (Iseki et al., 1999); rat *Osteopontin* (*Spp1*) is described (Oldberg et al., 1986); *Osteocalcin* (*Ocn*) and *Twist1* were from C. Loomis (Deckelbaum et al., 2006; Rice et al., 2000). A 1 kb full-length *Noggin* clone was sub-cloned from an Invitrogen BMAP EST clone.

Cell Proliferation

For *in vivo* BrdU incorporation, pregnant mice were injected with BrdU (100 μg/g body weight) and sacrificed 30 minutes later. Embryos were genotyped and processed as described for ISH. After drying and staining for Alp activity, slides were immunostained for BrdU using the Amersham anti-BrdU kit and either Vector MOM staining kit with VIP visualization of HRP activity, or immunofluorescent detection with anti-mouse Alexa488 conjugates. Sections were then stained with Hoechst 33258 nuclear dye, washed, and mounted with Dapko immunofluorescence medium. Total (Hoechst-stained) nuclei and Alp stain were visualized under the appropriate fluorescence, and BrdU-positive nuclei with white light or fluorescence. Photos of each component of each section were combined in Photoshop for nuclei counting. Four to seven alternate sections, separated by 60–100 μm, were used for each comparison, choosing sections from the same level within the coronal suture, as judged by overall orientation of the sections, between WT and *Fgfr2*$^{\text{S252W/+}}$ littermates, above the level of any fusion in *Fgfr2*$^{\text{S252W/+}}$ sutures. Nuclei were counted if they were within or immediately adjacent to the Alp signal of the OFs, within a 130 μm distance at E12.5–E13.5, when the OFs lack osteoid and proliferating cells are widespread within the bone anlagen, and within approximately 70 μm distance at E14.5–E16.5, when proliferating cells become more restricted to the leading edges of the OFs. Counts were made for both individual- i.e. frontal and parietal

-OFs, and for intervening sutural mesenchyme, when possible. For cultured cells, cells plated in 8-well chamber slides (LabTek, Nalgene-Nunc International) were labeled with BrdU (4 μg/ml) for 4 hours. The treated cells were fixed in 3.7% PFA, and permeabilized with 0.5% Triton in PBS for 5 min, followed by 1.5 M HCl for 15 min. After washing, analysis of BrdU incorporation was performed using an anti-BrdU monoclonal antibody (Amersham) followed by an anti–mouse/Cy3 conjugate (1:200; Molecular Probes). The frequency of S-phase cells was calculated as a ratio of BrdU-positive nuclei to the total Hoechst-stained nuclei.

TUNEL

Apoptosis was detected using the In Situ Cell Death Detection Kit, POD (Roche).

Reverse Transcription and real-time PCR

RNA was prepared using Trizol Reagent (Invitrogen, USA) from cultured cells, or dissected calvaria consisting of the frontal, parietal and interparietal bones cleared of extraneous membranes and snap-frozen in liquid nitrogen. RNA was purified with the RNeasy MinElute Cleanup Kit (Qiagen, USA). cDNA was prepared with the SuperScript First-Strand kit (Invitrogen). Real-time PCR of cDNA was performed with the LightCycler FastStart DNA master SYBR green 1 kit (Roche) on a Light Cycler system (Roche). Relative expression levels were calculated using the level of *β-actin* in each sample as a reference. PCR oligonucleotide sequences are available upon request.

Statistics

Results for cell proliferation and mRNA expression levels are presented as the mean ± standard error of the mean (SEM), and were analyzed using the unpaired, two-tailed Student's *t* test. Differences with a P value ≤ 0.05 were considered significant.

Tissue Culture

Primary calvarial osteoblasts were prepared, maintained, and immortalized as described previously (Mansukhani et al., 2000), but with the substitution of Dulbecco's modification of Eagle's medium (DMEM; Gibco BRL) for αMEM. Briefly, individual calvaria of newborn (P1) mice, consisting of the frontal, parietal, and interparietal bones, were aseptically dissected, stripped of associated membranes, and serially digested 5 times for 15 minutes each in a solution of collagenase/dispase to liberate osteoblasts. The first fraction was discarded and the remaining four were combined, washed, and plated for culture. For differentiation assays osteoblasts were plated at 10^5 cells/well in a 12-well plate; after 24 hours the medium was supplemented with 50 μg/ml L-ascorbic acid and 4 mM Glycerol-2-phosphate, changed every three days. Alp activity was detected using a kit according to the manufacturer's instructions (85L-2; Sigma-Aldrich).

Protein Preparation and Western Blotting

Cultured cells were lysed in RIPA buffer (10 mM, Tris-HCl, pH 7.2, 150 mM NaCl, 5 mM EDTA, 0.1% SDS, 1% Na deoxycholate, 1% NP-40) containing protease inhibitor cocktail (Complete Mini EDTA-free, Roche) and phosphatase inhibitors (sodium orthovanadate). For tissue protein, calvaria were isolated from newborn pups as described previously, snap frozen in liquid nitrogen, then homogenized in RIPA buffer using a Polytron tissue homogenizer (Kinematika, Switzerland). Protein concentration was determined with Bradford Protein Assay reagent (BioRad). Equal amounts of protein were resolved on a 9% SDS-PAGE gel. Proteins were electrotransferred to nitrocellulose membrane (Protran BS85, Whatman) and incubated with the specific antibodies. Proteins were visualized by ECL (Amersham). The antibodies used were against Fgfr2 (SC-122; Santa Cruz); phospho-β-catenin (#9561), phospho-Akt (#9217), total Akt (#9272), phospho-p38 (#9211) (Cell Signaling Technology); activated β-

catenin (ABC, #05-655, Upstate Biotechnology); β-catenin (#610153, BD Transduction); α-tubulin (T6074, Sigma-Aldrich); and actin (ab11003, Abcam).

RESULTS

The Apert mouse model was formed by a knock-in strategy, which created a mutated *Fgfr2*$^{Neo\text{S252W}}$ allele whose expression was suppressed by the presence of a *Neo* cassette (Chen et al., 2003). Full expression of this allele was restored by crossing *Fgfr2*$^{Neo\text{S252W/+}}$ heterozygotes with EIIa promoter-*Cre* transgenic mice to remove the *Neo* cassette and generate *Fgfr2*$^{\text{S252W/+}}$ offspring. Crosses of *Fgfr2*$^{Neo\text{S252W/+}}$ males with EIIa-*Cre* females gave obviously affected pups at birth, identifiable by a domed head and short face (Fig. 1A). Genotyping of tail DNA showed that affected offspring were invariably *Neo* negative, and these genotypes were used for subsequent analysis. Some litters were allowed to develop beyond birth; however, *Fgfr2*$^{\text{S252W/+}}$ animals always died within a few days, as opposed to the variable longevity related to strength of phenotype previously reported (Chen et al., 2003), but similar to the recent report of a second Apert syndrome mouse model (Wang et al., 2005). Furthermore, affected pups could often be identified morphologically as early as E13.5 and onwards, the back of the head being less rounded than in WT littermates (not shown). Mice were also out-bred with a Swiss Webster background, with no difference in phenotype noticed, and are included in the analyses. Occasionally, mosaic but viable animals having a domed head, short face and malocclusion were obtained, and were also used for breeding when fertile.

Coronal suture fusion is an early embryonic event

Inspection of newborn *Fgfr2*$^{\text{S252W/+}}$ skulls revealed extensive coronal suture fusion (Fig. 1B). The development of the coronal suture was therefore examined between E12.5 and P1, the period of embryonic skull formation. Alkaline phosphatase (Alp) activity, upregulated in pre-osteoblasts and osteoblasts (Candeliere et al., 2001), was visualized histochemically in intact embryos (E12.5, Fig. 1C) or transverse sections covering the entire calvaria (Fig. 1D). This showed the positions of osteogenic fronts (OFs) and areas of osteoid and bone (unmineralized and mineralized extracellular matrix, respectively). At E12.5 Alp staining showed slight individual variation between littermates but no clear differences between WT and *Fgfr2*$^{\text{S252W/+}}$ pups (Fig. 1C). In Fig. 1D we present the progress of coronal suture fusion at both the basal (ciliary region) and mid/upper levels of the suture. In the WT basal coronal suture the OFs lack osteoid until E15.5, when they also become more compact and tapered in shape. Unlike most of the coronal suture, the OFs do not overlap, but from E15.5 part of the parietal OF lies near forked ends of the frontal bone for a short distance. In *Fgfr2*$^{\text{S252W/+}}$ animals at E13.5 the gap between frontal and parietal OFs is already smaller, and by E14.5 is bridged by a uniform band of high Alp activity, at a point near to but above the lower limits of the frontal and parietal bones. At E15.5 the frontal and parietal osteoid is in close contact or continuous in at least one of the two coronal sutures, and is continuous in both sutures by E16.5 (Fig. 1D; n=6/6 pairs). The forked structure of the frontal bone in this region was not formed in the *Fgfr2*$^{\text{S252W/+}}$ suture.

In the mid-sutural region and higher, the WT OFs are closely opposed by E14.5, and develop the typical overlapped arrangement by E16.5, when they are also tapered and contain osteoid. In contrast, the *Fgfr2*$^{\text{S252W/+}}$ OFs were more closely opposed at E13.5 and showed a precocious deposition of osteoid by E15.5. They were generally more robust in appearance but still formed the overlapping arrangement by E16.5 along the remaining length of the suture, as in the WT. The extent of fusion seen in this region from E16.5 to P1 varied between *Fgfr2*$^{\text{S252W/+}}$ animals, but in contrast to the basal region, here suture fusion is between overlapping OFs containing osteoid (E16.5, P1, Fig. 1D; also Fig. 6). Also, the continued patency of much of the *Fgfr2*$^{\text{S252W/+}}$ coronal suture during this period, despite the closer approximation of the OFs,

indicates a much slower rate of fusion compared to the basal suture. Although fusion starts in the *Fgfr2*$^{S252W/+}$ basal suture and proceeds largely apically, in the apex of the suture points of fusion could occasionally be found above patent areas at P1 (not shown). A small amount of fusion also occurs downwards below the initial fusion point, towards the lower limit of the coronal suture.

These observations show that in *Fgfr2*$^{S252W/+}$ mice coronal suture fusion begins early in cranial development, with the coalescence of the frontal and parietal osteogenic mesenchymal domains near the base of the suture, and subsequent loss of the intervening sutural mesenchyme. The early rapid progress of the *Fgfr2*$^{S252W/+}$ OFs, and the precocious deposition of osteoid, further suggests that the early stages of osteoblast induction and maturation are accelerated.

Ectopic expression of genes related to osteoblast development

To determine the basis of premature suture fusion we used RNA ISH to examine the expression of genes characteristic of the OFs (*Fgfr1,−2*), osteoblast maturation (*Osteopontin*, *Spp1; Osteocalcin*, *Ocn*), and involved in suture patency (*Noggin*, *Twist1*), and assessed cell proliferation and apoptosis. In the WT, *Fgfr1* and *−2* become differentially expressed in osteoblasts at the OFs and along the developing bone surfaces, with a wider domain of *Fgfr2* expression encompassing the proliferating osteoprogenitors and a nested domain of *Fgfr1* expression occurring in more mature post-proliferative osteoblasts (Fig. 2A) (Iseki et al., 1999). This relationship was maintained in the mutant, but their expression also reflected the changes seen with Alp activity. While no differences were noted at E12.5 (not shown), at E13.5 the limits of *Fgfr2* and *−1* expression were closer in the *Fgfr2*$^{S252W/+}$ suture compared to the WT, with *Fgfr2* expression becoming continuous at their closest points of approximation (Fig. 2A).

Osteopontin and osteocalcin are markers of early and late osteoblast maturation, respectively (Candeliere et al., 2001), and their expression begins deep within the osteogenic domains before progressing outwards towards the OFs. The timing of *Spp1* expression was similar in WT and *Fgfr2*$^{S252W/+}$ calvaria, beginning at E14.5 in the frontal and parietal bones and by E15.5 in the inter-parietal bone (not shown) (Iseki et al., 1997). A major difference in expression was seen by E15.5 in the basal coronal suture very near or within regions of fused osteoid, where the leading edges of *Spp1* expression extended closer to each other in the *Fgfr2*$^{S252W/+}$ mouse (Fig. 2B). It should be noted that the osteoid was initially deposited by osteoblasts expressing *Fgfr1* but not *Spp1*. Continuous *Spp1* expression between frontal and parietal bones of *Fgfr2*$^{S252W/+}$ sutures, in conjunction with osteoid or mineralized bone, was seen from E15.5–E16.5 (not shown). Like *Spp1*, *Ocn* expression was more widespread in *Fgfr2*$^{S252W/+}$ calvaria in areas of early fusion (Fig. 2B). *Spp1* and *Ocn* expression was similar between WT and *Fgfr2*$^{S252W/+}$ animals in patent regions of the coronal suture (not shown).

The BMP inhibitor Noggin has been proposed as a regulator of suture patency. It can be down-regulated during FGF-induced craniosynostosis, and ectopic noggin expression can maintain suture patency (Warren et al., 2003). *Noggin* was expressed in the WT OFs and along the bone plates in a similar pattern to the *Fgfrs* (Fig. 2C). Generally, no difference other than its advanced expression in *Fgfr2*$^{S252W/+}$ OFs compared to WT sutures was seen. However, its expression did not decrease in advance of coronal suture fusion in the *Fgfr2*$^{S252W/+}$ mouse, but bridged the sutural mesenchyme separating the bone plates prior to fusion (Fig. 2C).

Inactivating mutations of the bHLH factor H-TWIST are responsible for Saethre-Chotzen syndrome in humans, involving coronal suture CS, and *Twist1*+/− mice also suffer coronal suture CS (Carver et al., 2002; el Ghouzzi et al., 1997; Howard et al., 1997). *Twist1* was expressed in immature skeletal mesenchyme, the OFs, and in sutural mesenchyme at E14.5 (Fig. 2D) and E15.5 (not shown). Apart from the more uniform expression of *Twist1* across

Fgfr2$^{S252W/+}$ coronal suture mesenchyme expressing Alp and *Fgfr2* before fusion, we found no differences in *Twist1* expression between WT and *Fgfr2*$^{S252W/+}$ calvaria.

In Fig. 3 the process of fusion is traced in a single *Fgfr2*$^{S252W/+}$ coronal suture at E15.5, progressing from the initial fusion point towards the base of the suture (Fig. 3B; see small arrow in Fig. 1B). Fusion is preceded by the advance of *Fgfr2* expression in the OFs into the sutural mesenchyme. Once the *Fgfr2*-expressing OFs meet and form a continuous sheet joining frontal and parietal mesenchyme, *Fgfr2* is down-regulated, *Fgfr1* continues to be expressed, and finally osteoid is deposited, obliterating the suture. *Fgfr2*-expressing osteoblasts are relegated to the surface of the new bone, contiguous with *Fgfr2*-expressing cells in the frontal and parietal bones. Grossly normal bone formation proceeds from this point. The WT sutural arrangement in this area is shown in Fig. 3A.

In mice carrying activating *Fgfr* mutations significant increases in the expression of osteoblast marker genes such as *Runx2*, *Spp1*, and *Ocn* prior to the time of fusion have been reported (Eswarakumar et al., 2004; Zhou et al., 2000). We compared the mRNA expression levels in WT and *Fgfr2*$^{S252W/+}$ calvaria of various genes relevant to the osteoblast phenotype and suture patency using quantitative real-time RTPCR. The stages examined were E15.5 (Fig. 4), when fusion is beginning but much of the coronal suture is open, and E17.5 (not shown), when coronal suture fusion is well advanced. No significant differences were seen in expression levels between WT and *Fgfr2*$^{S252W/+}$ calvaria of genes involved in OF function (*Fgfr1* and *−2* IIIc mesenchymal isoforms) or general osteoblast activity and differentiation (*Alp, Runx2, Col1a1*), or maturation (*Spp1*, *Ocn*, *Mepe*, *Sost*), although the expression of these latter genes was mildly elevated in *Fgfr2*$^{S252W/+}$ compared to WT calvaria at E15.5. These differences were smaller at E17.5, although loss of much of the suture at E17.5 would not of itself be expected to result in a large change in these expression levels as these genes are expressed in osteoblasts beyond the sutural zone. The results show that the Apert Fgfr2 mutation does not cause significantly higher steady-state expression levels of these genes in osteoblasts. The levels of *Noggin*, *Gdf6*, or *Twist1*, the loss of any of which is associated with synostosis, were not altered during the fusion process (as seen previously for *Noggin* and *Twist1*; Fig. 2C, D).

The expression patterns of genes in the developing calvarial bones confirms our initial finding of accelerated osteoblast induction and failure of the basal OFs to arrest their progress at the sutural mesenchyme. These changes occur without enhanced levels of osteoblast gene expression. Once a contiguous osteogenic domain is established in place of the sutural mesenchyme, a relatively normal sequence of bone formation occurs. Ectopic osteoid is deposited both between the frontal and parietal domains during their fusion, and in the higher unfused OFs of the *Fgfr2*$^{S252W/+}$ coronal suture.

Altered proliferation is not sufficient to account for suture fusion

The domain of *Fgfr2* expression in calvaria coincides with osteoblast proliferation (Iseki et al., 1999), and activated Fgfr2 signaling has been reported to increase cell proliferation *in vivo* (Eswarakumar et al., 2004). Cell proliferation in the coronal sutures of the WT and *Fgfr2*$^{S252W/+}$ mouse was assessed using pre-natal BrdU incorporation (Fig. 5) and by detecting Ki67 (not shown), with similar results. As the frontal and parietal bones are derived from neural crest and mesoderm, respectively (Jiang et al., 2002), proliferating cells were counted separately in each OF in case cell lineage-specific differences were present. In fusing *Fgfr2*$^{S252W/+}$ sutures, counts were performed in OFs above the level of fusion and compared to equivalent areas in WT sutures.

At E12.5 the frontal and parietal osteogenic fronts are widely separated both in WT and *Fgfr2*$^{S252W/+}$ animals (Fig. 1C). BrdU incorporation was consistently higher in *Fgfr2*$^{S252W/+}$ frontal and parietal regions compared to WT, though these differences were not

always statistically significant (Fig. 5A). No increase in the proportion of BrdU-positive cells was seen in *Fgfr2*$^{S252W/+}$ frontal or parietal OFs compared to WT between E13.5 and E14.5 (Fig. 5A), nor in the intervening sutural mesenchyme at E13.5 (not shown). At E15.5, comparing a WT suture to an *Fgfr2*$^{S252W/+}$ suture beginning to fuse, only a mildly greater proportion of BrdU-positive cells was seen in the WT frontal OF. At E16.5 a significant drop in BrdU-positive cells was seen in *Fgfr2*$^{S252W/+}$ sections above the region of fusion compared to WT (Fig. 5A). This difference at E16.5 was similar in six pairs compared (three each on the original and out-bred backgrounds). This decrease in proliferation was especially apparent in the region of the frontal and parietal OFs facing each other prior to fusion (Fig. 5B). No consistent differences in proliferation were seen between neural crest- and mesoderm-derived osteoblasts.

Thus, despite an initial increase, OF proliferation is not enhanced during basal sutural fusion, and abruptly decreases compared to the WT during later sutural fusion, perhaps reflecting accelerated maturation at the expense of proliferation occurring in the apical OFs in the *Fgfr2*$^{S252W/+}$ mice.

Apoptosis is secondary to suture fusion

In the initial report of this Apert mouse model, apoptosis was seen to be significantly higher in the post-natal *Fgfr2*$^{S252W/+}$ coronal suture compared to the WT, and it was proposed that this allowed sutural fusion (Chen et al., 2003). Apoptosis in the embryonic coronal suture is negligible before E17.5 (Bourez et al., 1997; Rice et al., 1999). We assessed apoptosis in the developing coronal suture by TUNEL. Before E16.5, few or no apoptotic cells were detected in either WT or *Fgfr2*$^{S252W/+}$ coronal sutures, despite their clear differences in sutural development, including those sutures at E15.5 where Alp activity between the frontal and parietal bones was continuous prior to or during osteoid deposition (not shown). At E16.5 apoptotic cells appeared in the *Fgfr2*$^{S252W/+}$ coronal sutures, but were strictly limited to sites of osteoid contact between the frontal and parietal bones and not seen in the more extended area of decreased proliferation above this point in the *Fgfr2*$^{S252W/+}$ coronal suture (Fig. 6). Apoptosis therefore appeared to be a consequence rather than a cause of sutural fusion in *Fgfr2*$^{S252W/+}$ mice.

Cartilage abnormalities in the *Fgfr2*$^{S252W/+}$ calvaria

Ectopic cartilage in the cranial vault was seen in the second Apert mouse model (Wang et al., 2005). We noted apical overgrowth of the orbito-sphenoid cartilage, and an ectopic pair of short cartilage bands in the sagittal suture in *Fgfr2*$^{S252W/+}$ mice at E16.5 (Supplemental Fig. 1). In contrast to the rapid suture closure we see in the *Fgfr2*$^{S252W/+}$ mouse, ectopic cranial cartilage can hinder suture formation (Holmbeck, 2005). In the *Fgfr2*$^{S252W/+}$ mouse any link between ectopic cartilage and coronal suture fusion is unknown, although fusion occurred in areas where the difference between WT and *Fgfr2*$^{S252W/+}$ cartilage was minimal (the early basal suture) or where cartilage did not occur (the upper suture).

Behavior of osteoblasts from *Fgfr2*$^{S252W/+}$ mice in culture

The experiments described in the preceding sections highlight a complex developmental scenario, in which the *Fgfr2*$^{S252W/+}$ mice showed a very early suture closure phenotype. Osteoblasts differentiated at an accelerated rate and did not respond to physiological signals that inhibit osteoblast induction in the suture. A slight increase in the number of proliferating osteoblasts in OFs was observed at early stages of embryonic development (E12.5). To better understand the dynamics of osteoblast proliferation and differentiation determining Fgfr2-induced craniosynostosis, we examined the behavior of osteoblasts isolated from the calvarial of *Fgfr2*$^{S252W/+}$ mice and WT littermates in culture. Primary calvarial osteoblasts were isolated from pure P1 *Fgfr2*$^{S252W/+}$ and from WT littermate mice. The genotype of the cultured cells

was verified by PCR (data not shown). In some cases, these cells were immortalized by infection with a retroviral vector expressing the polyoma large T-Ag (LT).

Fgfr2$^{S252W/+}$ cells proliferate faster in culture

BrdU incorporation studies demonstrated that primary osteoblast cultures isolated from *Fgfr2*$^{S252W/+}$ mice divide at a significantly higher rate than cells isolated from WT littermates (Fig. 7A). P1 calvarial osteoblasts from a different pair of *Fgfr2*$^{S252W/+}$ and WT littermate mice were also examined after LT immortalization. BrdU incorporation showed that the *Fgfr2*$^{S252W/+}$ cells have a higher rate of DNA synthesis than the WT. Addition of 5 or 20 ng/ml recombinant FGF1 to the culture medium increased proliferation of all cells but did not alter the ratio of BrdU incorporation between WT and *Fgfr2*$^{S252W/+}$ cells (Fig. 7A, B). A growth curve (Fig. 7C) also showed a significantly faster rate of growth of *Fgfr2*$^{S252W/+}$ relative to the WT cells.

Accelerated differentiation of *Fgfr2*$^{S252W/+}$ cells in culture

Calvarial osteoblasts isolated from a P1 *Fgfr2*$^{S252W/+}$ and a WT littermate were cultured in differentiation medium and stained at regular intervals for Alp. Fig. 8A demonstrates that the *Fgfr2*$^{S252W/+}$ osteoblasts stained positive for Alp earlier and more strongly than the WT littermate osteoblasts. We and others previously showed that Akt activation promotes osteoblast differentiation (Kawamura et al., 2007;Raucci et al., 2008). By Western blot we showed that phospho-Akt is upregulated in *Fgfr2*$^{S252W/+}$ osteoblasts in comparison to WT osteoblasts (Fig. 8B), consistent with an increased ability to differentiate. As also noted previously, osteoblasts expressing increased levels of phospho-Akt have increased amounts of activated β-catenin, a central molecule in Wnt signaling, which promotes osteoblast differentiation (Raucci et al., 2008). In line with the observation that *Fgfr2*$^{S252W/+}$ cells differentiate faster, they had decreased levels of phospho-β-catenin and high levels of active β-catenin. (Fig. 8B). Increased phospho-Akt was also detected in calvarial tissues of two *Fgfr2*$^{S252W/+}$ animals, along with increased phospho-p38 (Fig. 5B), another positive regulator of osteoblast differentiation (Hu et al., 2003).

To confirm the increased rate of differentiation of *Fgfr2*$^{S252W/+}$ osteoblasts, we used LT immortalized calvarial osteoblasts isolated from newborn *Fgfr2*$^{NeoS252W/+}$ mice, which contain the *Neo* cassette upstream of the Apert S252W mutation. These mice carry the Apert mutation but the presence of the *Neo* cassette compromises its expression. These cells were divided into two populations and infected with the pLXS-Cre-EGFP virus (designed to excise the *Neo* cassette) or with the pLXS-EGFP virus only. Fig. 8C shows successful excision of the *Neo* cassette from a majority of the cells after infection with the *Cre*-containing virus, which also resulted in increased expression of *Fgfr2* mRNA. After 14 days in differentiation medium cells infected with the *Cre* virus stained strongly for Alp, indicating that they differentiate faster than control cells, while WT osteoblasts did not show any difference in Alp expression between *Cre*-infected and uninfected cells (data not shown). We measured the expression of several osteoblast differentiation markers at various times after infection with the *Cre* or the control virus. *Cre*-infected cells expressing activated Fgfr2 showed a strong increase in the expression of *Col1a1, Runx2, Alp,* and *Timp3* mRNAs relative to the controls (Fig. 8D). Thus, the expression of activated Fgfr2 results in faster osteoblastic differentiation.

It has been widely observed that prolonged treatment of osteoblasts in culture with exogenous FGF prevents differentiation (Mansukhani et al., 2000; Tang et al., 1996). We therefore examined the response of *Fgfr2*$^{S252W/+}$ and WT osteoblasts to exogenous FGF1. *Fgfr2*$^{S252W/+}$ and WT cells continuously incubated with 10 μg/ml of FGF1 did not differentiate even after 14 days in differentiation medium. A dose-response experiment showed that no concentration of exogenous FGF1 could accelerate differentiation, with the response varying

from no effect to complete inhibition of differentiation. Thus *Fgfr2*$^{S252W/+}$ cells respond to exogenous FGF as their WT counterpart (data not shown).

Expression of Fgfr2 and Fgfr1 in *Fgfr2*$^{S252W/+}$ and WT cells

It has been proposed that downregulation of Fgfr2 expression during *in vivo* osteoblast development allows signaling from Fgfr1 and osteogenic differentiation (Morriss-Kay and Wilkie, 2005). It has also been reported that human Apert osteoblasts express low levels of Fgfr2 protein in culture (Lemonnier et al., 2000). We therefore determined the levels of expression of Fgfr1 and Fgfr2 in several matched cultures of WT and *Fgfr2*$^{S252W/+}$ osteoblasts derived from newborn litters. While the expression levels of Fgfr1 were similar in all samples, we found a variable reduction in the expression of Fgfr2, both at the RNA and protein level, in *Fgfr2*$^{S252W/+}$ compared to WT osteoblasts, varying from about 20% of the matched WT osteoblasts, to levels only slightly lower (70–80%) (Supplemental Fig. 2A). It has been shown that FGF signaling downregulates the expression of Fgfr2, but not of Fgfr1, in several cell types (Ali et al., 1995), and we therefore determined whether this was also the case in osteoblasts. FGF treatment of both WT and *Fgfr2*$^{S252W/+}$ osteoblasts strongly reduced the expression of both Fgfr2 RNA and protein, while expression of Fgfr1 was not significantly affected (Supplemental Fig. 2B). We therefore consider it likely that the variable downregulation of Fgfr2 expression observed in *Fgfr2*$^{S252W/+}$ osteoblasts could be due to a degree of autocrine FGF signaling taking place in these cells. Since the major activating effect of the Apert S252W mutation is to increase and broaden FGFR2 affinity for FGF ligands (Yu et al., 2000), endogenous production of low amounts of Fgf could downregulate Fgfr2 expression. Because of the downregulation of Fgfr2 expression, all *Fgfr2*$^{S252W/+}$ cells had relatively higher levels of Fgfr1 versus Fgfr2 than WT cells.

DISCUSSION

How the cranial sutures are initially established and the integrity of the sutural mesenchyme between bone fronts subsequently maintained is not clearly understood. FGF, TGFβs, and BMPs, expressed in both the osteogenic mesenchyme and underlying dura mater, all regulate suture patency (Opperman, 2000). Expression studies and the application of FGF to cultured crania has shown a correlation between low FGF levels, *Fgfr2* expression, and osteoblast proliferation on the one hand, and between high FGF levels, *Fgfr1* expression, and osteoblast differentiation on the other (Iseki et al., 1997; Iseki et al., 1999). At the OFs and along the bone surfaces, there is a general progression with increasing maturation from proliferating osteoprogenitors expressing *Fgfr2* to post-proliferative osteoblasts expressing *Fgfr1*, and mature osteoblasts may express neither receptor (Iseki et al., 1999; Johnson et al., 2000). It is hypothesized that FGF signals drive the progress of the OFs, and that suture patency is controlled, at least in part, by the influence of an FGF gradient on the balance between osteoblast proliferation and differentiation, with aberrant FGF signaling triggering a switch from *Fgfr2* expression and proliferation to *Fgfr1* expression and differentiation, ultimately resulting in suture fusion (Morriss-Kay and Wilkie, 2005).

Despite the variety of murine models of deleted or activated Fgfr2 available, a description of the initiation and progress of coronal suture fusion, or a consensus on how activated Fgfr2 causes it, is lacking. Targeted deletion of *Fgfr2* in osteoblasts shows that it is not entirely essential for proliferation in the OFs (Eswarakumar et al., 2002; Yu et al., 2003), while the proliferative effects of activated Fgfr2 reported in the embryonic coronal suture were either transient in a Crouzon C342Y model (Eswarakumar et al., 2004) or undetected in the Apert model studied in this report (Chen et al., 2003). In mice with deleted or activated Fgfr2, differentiation was also decreased or enhanced, respectively (Eswarakumar et al., 2004; Eswarakumar et al., 2002). Furthermore, almost all models show post-natal coronal CS, but

the relationship of this later fusion to earlier embryonic changes is not clear. Embryonic CS has been seen in only one mouse model, in which ablation of the mesenchymal isoform Fgfr2-IIIc resulted in ectopic expression of the epithelial isoform Fgfr2-IIIb in osteoblasts, but the process of fusion was not described (Hajihosseini et al., 2001). The previous description of the mice studied in this report (Chen et al., 2003) noted a variable phenotype and viability of affected mice and only post-natal fusion of the coronal suture, which is at odds with our findings. This suggests that some of these mice were variably chimeric due to inefficient Cre activity, which may allow a much longer period of suture patency before fusion occurs.

In our study of this Apert model, we found CS to begin very early in cranial development. Near the base of the *Fgfr2*$^{S252W/+}$ coronal suture, the frontal and parietal osteogenic domains rapidly coalesce between E13.5–E15.5, as seen in the successive convergence of the expression domains of *Fgfr2*, followed by Alp, and then *Fgfr1*. It appears as if the two osteogenic domains simply advance until they join each other, with no formal separation ever being established. Osteoid is then deposited within a continuous osteogenic layer to join the two bones, and grossly normal bone formation follows. Perhaps surprisingly, further up the coronal suture the OFs form the increasingly more compact wedges of proliferating cells, post-proliferative osteoblasts, and osteoid, with the overlap typical of the WT suture. In contrast to the rapid fusion of soft mesenchyme in the basal suture, sutural fusion occurs from E15.5 between the tip of each remaining OF and the opposing osteoid, progressing apically but at a much slower rate than occurred in the basal suture. Enhanced osteoblast maturation is also seen in the developing *Fgfr2*$^{S252W/+}$ coronal suture, with the precocious deposition of osteoid across the sutural mesenchyme and in the more apical unfused OFs.

Analysis of proliferation showed a modest increase at E12.5 in the *Fgfr2*$^{S252W/+}$ suture. From E13.5–E14.5 in *Fgfr2*$^{S252W/+}$ basal sutural areas ectopic expression of Alp and *Fgfr2* is accompanied by ectopic proliferation. In the separate OFs above this, no difference is seen compared to the WT, suggesting that the increased advance of the OFs is not driven by increased proliferation. Further, as fusion continues in the *Fgfr2*$^{S252W/+}$ OFs higher in the suture at E16.5, there is a significant decrease in proliferation. This is likely to be the consequence of the shift towards greater osteoblast maturation occurring in the *Fgfr2*$^{S252W/+}$ suture at this time.

Apoptosis has been proposed as a mechanism to both prevent and promote suture fusion (Dry et al., 2001; Furtwangler et al., 1985; Rice et al., 1999). In the initial report of the mice used in the present study, increased post-natal apoptosis was proposed as the possible mechanism of suture fusion (Chen et al., 2003). Apoptosis also occurs during normal post-natal mid-line suture fusion (Fong et al., 2004). As we found it occurs as a late event in *Fgfr2*$^{S252W/+}$ sutural fusion, it is likely to be a consequence rather than a cause of synostosis.

The primary event of suture fusion that must be understood in the *Fgfr2*$^{S252W/+}$ mouse is the failure of the OFs to halt their progress across a discreet distance of sutural mesenchyme in the basal suture. *Fgfr2* is expressed at a low level throughout this mesenchyme, rising in level at the OFs (Johnson et al., 2000). In the normal coronal suture, a key role in halting the progress of OFs is played by the bHLH factor, Twist1, which is expressed in sutural mesenchyme, OFs, and immature skeletal mesenchyme (Bialek et al., 2004; Connerney et al., 2006; Johnson et al., 2000; Rice et al., 2000). Haploinsufficiency of H-TWIST in humans is the cause of coronal suture fusion in Saethre-Chotzen syndrome (el Ghouzzi et al., 1997; Howard et al., 1997), and in mice with an inactivating *Twist1* mutation causing CS (Carver et al., 2002) ectopic induction of *Fgfr2* is seen in sagittal and coronal sutural mesenchyme (Connerney et al., 2008; Connerney et al., 2006; Rice et al., 2000). The control of *Fgfr2* expression by Twist1 is complex, involving a balance between Twist1 homodimers, which activate *Fgfr2* expression in the OFs, and Twist1/E-protein heterodimers, which repress *Fgfr2* expression in the sutural mesenchyme (Connerney et al., 2008; Connerney et al., 2006); furthermore, Fgf signaling can upregulate

Twist1 expression (Rice et al., 2000). A simple scenario in the *Fgfr2*$^{S252W/+}$ coronal suture is that excessive Fgfr2 activation in the suture mesenchyme overcomes the suppressive Twist-based (or other) signal, allowing conversion to the osteoblast fate, with the resulting loss of the suture. This possibility is supported by the finding that in the *Twist1*+/− mouse, suppression of wild-type Fgfr2 activity is enough to prevent CS (Connerney et al., 2008), which suggests that the efficacy of Twist1 function depends on the relative strength of Fgfr2 signaling. This mechanism would not require enhanced osteoblast proliferation or apoptosis in the *Fgfr2*$^{S252W/+}$ mutant, or changes in *Twist1* expression, none of which were observed during the early period of suture fusion. The heightened sensitivity of mutant Fgfr2 to Fgfs would also explain why the OFs of the *Fgfr2*$^{S252W/+}$ calvaria advance more rapidly compared to the WT OFs prior to suture fusion. Another similarity between the *Fgfr2*$^{S252W/+}$ and *Twist1*+/− mice is the appearance of Alp-expressing cells within sutural mesenchyme at E14.5 in the *Twist1*+/− coronal suture (Merrill et al., 2006). These authors showed disruption of the neural crest/mesoderm boundary between frontal and parietal domains and mixing of the cell lineages. While the contribution of this mixing to CS is unknown, its possible occurrence in the *Fgfr2*$^{S252W/+}$ mouse would be an important avenue of investigation.

Noggin has also been proposed to act as a brake on OF expansion, its presence limiting the promotion of differentiation by BMPs. FGF signaling can down-regulate noggin expression, allowing differentiation of the suture mesenchyme across a post-natal suture (Warren et al., 2003). However, we did not see down-regulation of *Noggin* at the OFs prior to suture fusion, and its role in embryonic sutural development is still unknown.

While calvarial osteogenic mesenchyme is generally thought to arise from within the dermal membrane by induction and recruitment of cells to the osteoblast fate, recent evidence suggests that it arises within a separate skeletogenic mesenchyme established by the proliferation and migration of independent cell populations from the baso-lateral regions of the calvaria (Yoshida et al., 2008). While cell migration was apparent at E13.5, it is not yet clear whether the OFs represent the frontier of these migrating and proliferating cells, or mark a secondary wave of osteoblast induction and growth once the skeletogenic mesenchyme is in place. In the former case, activated Fgfr2 must act in the *Fgfr2*-expressing osteoprogenitors to overcome a signal that prevents their expansion into the sutural mesenchyme. The mildly higher proliferation of frontal and parietal *Fgfr2*$^{S252W/+}$ osteoblasts at E12.5 and their closer approximation by E13.5 may therefore represent an early enhancement of osteoblast expansion by Fgfr2 signaling in the *Fgfr2*$^{S252W/+}$ calvaria.

The failure of basal suture formation is in contrast to the ability of *Fgfr2*$^{S252W/+}$ osteoblasts in the higher suture to respond to developmental cues and initially form the appropriate sutural architecture, which persists to varying degrees, despite the similar closer approximation of the OFs. This suggests that the processes of suture formation and fusion differ significantly between the basal and higher suture, or may reflect a change in the interactions of suture mesenchyme and osteoblasts as the OFs change from a rapidly expanding soft mesenchyme to a compact mineralizing osteoid. However, the *Fgfr2*$^{S252W/+}$ osteoblasts in the upper suture do behave abnormally. Prior to fusion proliferation markedly decreases in the remaining suture at E16.5 compared to the WT, while maturation, as suggested by the increased deposition of osteoid, is enhanced, suggesting a shift in the balance between proliferation and differentiation in the OFs. Given that the expression domains of *Fgfr2* and *Spp1* are mutually exclusive (Iseki et al., 1997), and that osteoid is initially deposited by osteoblasts expressing *Fgfr1* but not *Spp1*, it is likely that the activated Fgfr2 signaling specifically enhances early osteoblast maturation, perhaps by speeding the progression to *Fgfr1* expression.

Coronal suture development in the *Fgfr2*$^{S252W/+}$ mouse bears striking similarities to the human Apert suture pathology. The early fetal occurrence of Apert sutural fusion (Kreiborg and

Cohen, 1990) and the progressive nature of coronal suture fusion from an inferior location (Albright and Byrd, 1981) have been noted. In particular, the late fetal *Fgfr2*$^{S252W/+}$ murine coronal suture is very similar to that of the fetal Apert skull shown by Mathijssen et al (Mathijssen et al., 1996), where sutural agenesis and osseous obliteration occur in the basal portion of the coronal suture but a recognizable suture is formed both in the upper suture and at its very base. These similarities between the *Fgfr2*$^{S252W/+}$ mouse and human Apert syndrome suggest that this Apert mouse model is a promising model for developing preventative therapies against CS, and it has already been used to assess the effectiveness of MEK inhibitors, which reduce ERK activation and therefore FGF signaling (Shukla et al., 2007). While it might be thought that the early synostosis alone could constrain later sutural growth and ensure continued fusion, this study showed that synostosis is an ongoing process and that mature sutures can still fuse even if the early synostosis is minimized or prevented by treatment with FGF signaling inhibitors *in utero* (Shukla et al., 2007). The enhanced osteoblast activity in the OFs of the mature mutant coronal sutures seen in our study is in line with this finding.

To better understand the intrinsic alterations in osteoblasts caused by the expression of activated Fgfr2, we cultured primary osteoblasts from the calvaria of WT and *Fgfr2*$^{S252W/+}$ mice. We found that *Fgfr2*$^{S252W/+}$ cells clearly proliferate faster than the WT, and showed an increased ability to differentiate, in agreement with findings from similar osteoblasts derived from the second Apert mouse model (Yang et al., 2008). The increased proliferation of *Fgfr2*$^{S252W/+}$ cells in culture supports the notion that the slight increase in BrdU incorporation observed *in vivo* at E12.5 could contribute to the accelerated suture closure in *Fgfr2*$^{S252W/+}$ mice. Similarly, the increased ability to differentiate, that has also been observed in other laboratories in both human Apert (Lomri et al., 1998) and mouse *Fgfr2*$^{S252W/+}$ osteoblasts (Yang et al., 2008), is consistent with the accelerated maturation of osteoblasts in the basal and higher coronal suture.

How aberrant FGF signaling from the Apert Fgfr2 would promote both proliferation and differentiation, seemingly antithetic processes, is still unclear. Since it has been proposed that in osteoblasts, Fgfr2 signaling is linked to proliferation and Fgfr1 to differentiation, we explored whether the levels of expression of these receptors correlated with the increased ability of *Fgfr2*$^{S252W/+}$ cells to differentiate. While the levels of Fgfr1 expression appeared rather uniform, we found a variable reduction of Fgfr2 expression in *Fgfr2*$^{S252W/+}$ cells in comparison to WT controls. This is likely due to the downregulation of Fgfr2 expression by some degree of autocrine FGF signaling in these cells, a notion supported by the finding that treatment of *Fgfr2*$^{S252W/+}$ osteoblasts with the Fgfr inhibitor SU5402 increased expression of Fgfr2 (G. R. and C. B. unpublished results). The accelerated differentiation of *Fgfr2*$^{S252W/+}$ cells in culture is in contrast to the behavior of osteoblasts transfected to express high and unregulated levels of activated Fgfr2, which are strongly inhibited in differentiation (Mansukhani et al., 2000), and tends to support the hypothesis that high levels of Fgfr2 signaling promote osteoblast proliferation and inhibit differentiation. In culture, Fgfr1 is expressed at higher levels than Fgfr2 in all osteoblast WT cultures we examined. Since Fgfr2 expression is also reduced further in *Fgfr2*$^{S252W/+}$ cells, this could argue in favor of the hypothesis that the relative increase in Fgfr1 expression could play a role in accelerating osteoblast maturation in *Fgfr2*$^{S252W/+}$ versus WT cells.

In conclusion, our studies highlight a complex process of FGF-induced craniosynostosis that occurs very early in embryonic cranial development. Sutural mesenchyme cells and/or osteoprogenitor cells in the OFs expressing activated Fgfr2 do not respond to signals that prevent osteoblast induction in the presumptive suture. Osteoprogenitor cells expressing the Apert mutation have an intrinsic ability to proliferate faster than the WT, a property easily detected in culture, but which is only observed at very early developmental times *in vivo*, probably because of the presence of other contrasting signals. These cells also differentiate

faster both *in vitro* and *in vivo*, so that we observe a premature and uncontrolled appearance of mature osteoblasts where normally the presence of undifferentiated mesenchyme marks the suture. Presently, the prevailing notion of how cranial OFs advance and the skull bones are formed is that undifferentiated cells in the suture mesenchyme are recruited or induced to assume the osteoblastic fate. It has however been recently proposed that osteoprogenitor cells, derived from bone primordia in the base of the skull, advance and migrate into the suture mesenchyme until an appropriate stimulus halt their progression. In either case our results strongly support the notion that the critical event in FGFR2-induced craniosynostosis is the failure to respond to stimuli that would halt the recruitment or the advancement of osteoprogenitor cells at the sites where sutures should normally form. Once past this "point of no return," a relatively normal progression of osteoblast differentiation and bone formation occurs.

Supplementary Material

Refer to Web version on PubMed Central for supplementary material.

Acknowledgements

We thank Ron Deckelbaum for helpful discussions, Lisa Dailey for critical reading of the manuscript, and Gillian Morriss-Kay and Cynthia Loomis for plasmids. Technical assistance was provided by the NYU Langone Research Histology Core. This investigation was supported by PHS grant AR051358 from the NIAMS.

References

Albright AL, Byrd RP. Suture pathology in craniosynostosis. J Neurosurg 1981;54:384–7. [PubMed: 7463140]

Ali J, Mansukhani A, Basilico C. Fibroblast growth factor receptors 1 and 2 are differentially regulated in murine embryonal carcinoma cells and in response to fibroblast growth factor-4. J Cell Physiol 1995;165:438–48. [PubMed: 7593222]

Bialek P, Kern B, Yang X, Schrock M, Sosic D, Hong N, Wu H, Yu K, Ornitz DM, Olson EN, Justice MJ, Karsenty G. A twist code determines the onset of osteoblast differentiation. Developmental Cell 2004;6:423–35. [PubMed: 15030764]

Bourez RL, Mathijssen IM, Vaandrager JM, Vermeij-Keers C. Apoptotic cell death during normal embryogenesis of the coronal suture: early detection of apoptosis in mice using annexin V. The Journal of craniofacial surgery 1997;8:441–5. [PubMed: 9477828]

Candeliere GA, Liu F, Aubin JE. Individual osteoblasts in the developing calvaria express different gene repertoires. Bone 2001;28:351–61. [PubMed: 11336915]

Carver EA, Oram KF, Gridley T. Craniosynostosis in Twist heterozygous mice: a model for Saethre-Chotzen syndrome. Anat Rec 2002;268:90–2. [PubMed: 12221714]

Chen L, Li D, Li C, Engel A, Deng CX. A Ser252Trp [corrected] substitution in mouse fibroblast growth factor receptor 2 (Fgfr2) results in craniosynostosis. Bone 2003;33:169–78. [PubMed: 14499350]

Cohen MM, Kreiborg S. Suture formation, premature sutural fusion, and suture default zones in Apert syndrome. Am J Med Genet 1996;62:339–44. [PubMed: 8723061]

Connerney J, Andreeva V, Leshem Y, Mercado MA, Dowell K, Yang X, Lindner V, Friesel RE, Spicer DB. Twist1 homodimers enhance FGF responsiveness of the cranial sutures and promote suture closure. Dev Biol 2008;318:323–34. [PubMed: 18471809]

Connerney J, Andreeva V, Leshem Y, Muentener C, Mercado MA, Spicer DB. Twist1 dimer selection regulates cranial suture patterning and fusion. Dev Dyn 2006;235:1345–57. [PubMed: 16502419]

Deckelbaum RA, Majithia A, Booker T, Henderson JE, Loomis CA. The homeoprotein engrailed 1 has pleiotropic functions in calvarial intramembranous bone formation and remodeling. Development 2006;133:63–74. [PubMed: 16319118]

Dry GM, Yasinskaya YI, Williams JK, Ehrlich GD, Preston RA, Hu FZ, Gruss JS, Ellenbogen RG, Cunningham ML. Inhibition of apoptosis: a potential mechanism for syndromic craniosynostosis. Plast Reconstr Surg 2001;107:425–32. [PubMed: 11214058]

el Ghouzzi V, Le Merrer M, Perrin-Schmitt F, Lajeunie E, Benit P, Renier D, Bourgeois P, Bolcato-Bellemin AL, Munnich A, Bonaventure J. Mutations of the TWIST gene in the Saethre-Chotzen syndrome. Nat Genet 1997;15:42–6. [PubMed: 8988167]

Eswarakumar VP, Horowitz MC, Locklin R, Morriss-Kay GM, Lonai P. A gain-of-function mutation of Fgfr2c demonstrates the roles of this receptor variant in osteogenesis. Proc Natl Acad Sci USA 2004;101:12555–60. [PubMed: 15316116]

Eswarakumar VP, Monsonego-Ornan E, Pines M, Antonopoulou I, Morriss-Kay GM, Lonai P. The IIIc alternative of Fgfr2 is a positive regulator of bone formation. Development 2002;129:3783–93. [PubMed: 12135917]

Fong K, Song H, Nacamuli R, Franc BL, Mari C, Fang T, Warren SM, Contag CH, Blankenberg FG, Longaker MT. Apoptosis in a rodent model of cranial suture fusion: in situ imaging and gene expression analysis. Plast Reconstr Surg 2004;113:2037–47. [PubMed: 15253194]

Furtwangler JA, Hall SH, Koskinen-Moffett LK. Sutural morphogenesis in the mouse calvaria: the role of apoptosis. Acta Anat (Basel) 1985;124:74–80. [PubMed: 4072611]

Hajihosseini MK, Wilson S, De Moerlooze L, Dickson C. A splicing switch and gain-of-function mutation in FgfR2-IIIc hemizygotes causes Apert/Pfeiffer-syndrome-like phenotypes. Proc Natl Acad Sci USA 2001;98:3855–60. [PubMed: 11274405]

Holmbeck K. Collagenase in cranial morphogenesis. Cells Tissues Organs 2005;181:154–65. [PubMed: 16612081]

Howard TD, Paznekas WA, Green ED, Chiang LC, Ma N, Ortiz de Luna RI, Garcia Delgado C, Gonzalez-Ramos M, Kline AD, Jabs EW. Mutations in TWIST, a basic helix-loop-helix transcription factor, in Saethre-Chotzen syndrome. Nat Genet 1997;15:36–41. [PubMed: 8988166]

Hu Y, Chan E, Wang SX, Li B. Activation of p38 mitogen-activated protein kinase is required for osteoblast differentiation. Endocrinology 2003;144:2068–74. [PubMed: 12697715]

Iseki S, Wilkie AO, Heath JK, Ishimaru T, Eto K, Morriss-Kay GM. Fgfr2 and osteopontin domains in the developing skull vault are mutually exclusive and can be altered by locally applied FGF2. Development 1997;124:3375–84. [PubMed: 9310332]

Iseki S, Wilkie AO, Morriss-Kay GM. Fgfr1 and Fgfr2 have distinct differentiation- and proliferation-related roles in the developing mouse skull vault. Development 1999;126:5611–20. [PubMed: 10572038]

Jiang X, Iseki S, Maxson RE, Sucov HM, Morriss-Kay GM. Tissue origins and interactions in the mammalian skull vault. Developmental Biology 2002;241:106–16. [PubMed: 11784098]

Johnson D, Iseki S, Wilkie AO, Morriss-Kay GM. Expression patterns of Twist and Fgfr1, -2 and -3 in the developing mouse coronal suture suggest a key role for twist in suture initiation and biogenesis. Mech Dev 2000;91:341–5. [PubMed: 10704861]

Kawamura N, Kugimiya F, Oshima Y, Ohba S, Ikeda T, Saito T, Shinoda Y, Kawasaki Y, Ogata N, Hoshi K, Akiyama T, Chen WS, Hay N, Tobe K, Kadowaki T, Azuma Y, Tanaka S, Nakamura K, Chung UI, Kawaguchi H. Akt1 in osteoblasts and osteoclasts controls bone remodeling. PLoS ONE 2007;2:e1058. [PubMed: 17957242]

Kreiborg S, Cohen MM Jr. Characteristics of the infant Apert skull and its subsequent development. J Craniofac Genet Dev Biol 1990;10:399–410. [PubMed: 2074277]

Lemonnier J, Delannoy P, Hott M, Lomri A, Modrowski D, Marie PJ. The Ser252Trp fibroblast growth factor receptor-2 (FGFR-2) mutation induces PKC-independent downregulation of FGFR-2 associated with premature calvaria osteoblast differentiation. Experimental Cell Research 2000;256:158–67. [PubMed: 10739663]

Lomri A, Lemonnier J, Hott M, de Parseval N, Lajeunie E, Munnich A, Renier D, Marie PJ. Increased calvaria cell differentiation and bone matrix formation induced by fibroblast growth factor receptor 2 mutations in Apert syndrome. J Clin Invest 1998;101:1310–7. [PubMed: 9502772]

Mansukhani A, Bellosta P, Sahni M, Basilico C. Signaling by fibroblast growth factors (FGF) and fibroblast growth factor receptor 2 (FGFR2)-activating mutations blocks mineralization and induces apoptosis in osteoblasts. J Cell Biol 2000;149:1297–308. [PubMed: 10851026]

Marie PJ, Coffin JD, Hurley MM. FGF and FGFR signaling in chondrodysplasias and craniosynostosis. J Cell Biochem 2005;96:888–96. [PubMed: 16149058]

Marie PJ, Debiais F, Hay E. Regulation of human cranial osteoblast phenotype by FGF-2, FGFR-2 and BMP-2 signaling. Histol Histopathol 2002;17:877–85. [PubMed: 12168799]

Mathijssen IM, Vaandrager JM, van der Meulen JC, Pieterman H, Zonneveld FW, Kreiborg S, Vermeij-Keers C. The role of bone centers in the pathogenesis of craniosynostosis: an embryologic approach using CT measurements in isolated craniosynostosis and Apert and Crouzon syndromes. Plast Reconstr Surg 1996;98:17–26. [PubMed: 8657773]

Merrill AE, Bochukova EG, Brugger SM, Ishii M, Pilz DT, Wall SA, Lyons KM, Wilkie AO, Maxson RE. Cell mixing at a neural crest-mesoderm boundary and deficient ephrin-Eph signaling in the pathogenesis of craniosynostosis. Hum Mol Genet 2006;15:1319–28. [PubMed: 16540516]

Miao D, Scutt A. Histochemical localization of alkaline phosphatase activity in decalcified bone and cartilage. J Histochem Cytochem 2002;50:333–40. [PubMed: 11850436]

Morriss-Kay GM, Wilkie AO. Growth of the normal skull vault and its alteration in craniosynostosis: insights from human genetics and experimental studies. J Anat 2005;207:637–53. [PubMed: 16313397]

Oldberg A, Franzen A, Heinegard D. Cloning and sequence analysis of rat bone sialoprotein (osteopontin) cDNA reveals an Arg-Gly-Asp cell-binding sequence. Proc Natl Acad Sci U S A 1986;83:8819–23. [PubMed: 3024151]

Opperman LA. Cranial sutures as intramembranous bone growth sites. Dev Dyn 2000;219:472–85. [PubMed: 11084647]

Ornitz DM. FGF signaling in the developing endochondral skeleton. Cytokine Growth Factor Rev 2005;16:205–13. [PubMed: 15863035]

Ornitz DM, Marie PJ. FGF signaling pathways in endochondral and intramembranous bone development and human genetic disease. Genes Dev 2002;16:1446–65. [PubMed: 12080084]

Raucci A, Bellosta P, Grassi R, Basilico C, Mansukhani A. Osteoblast proliferation or differentiation is regulated by relative strengths of opposing signaling pathways. J Cell Physiol 2008;215:442–51. [PubMed: 17960591]

Rice DP, Aberg T, Chan Y, Tang Z, Kettunen PJ, Pakarinen L, Maxson RE, Thesleff I. Integration of FGF and TWIST in calvarial bone and suture development. Development 2000;127:1845–55. [PubMed: 10751173]

Rice DP, Kim HJ, Thesleff I. Apoptosis in murine calvarial bone and suture development. Eur J Oral Sci 1999;107:265–75. [PubMed: 10467942]

Shukla V, Coumoul X, Wang R, Kim H, Deng CX. RNA interference and inhibition of MEK-ERK signaling prevent abnormal skeletal phenotypes in a mouse model of craniosynostosis. Nat Genet 2007;39:1145–50. [PubMed: 17694057]

Tang KT, Capparelli C, Stein JL, Stein GS, Lian JB, Huber AC, Braverman LE, DeVito WJ. Acidic fibroblast growth factor inhibits osteoblast differentiation in vitro: altered expression of collagenase, cell growth-related, and mineralization-associated genes. J Cell Biochem 1996;61:152–66. [PubMed: 8726364]

Wang Y, Xiao R, Yang F, Karim BO, Iacovelli AJ, Cai J, Lerner CP, Richtsmeier JT, Leszl JM, Hill CA, Yu K, Ornitz DM, Elisseeff J, Huso DL, Jabs EW. Abnormalities in cartilage and bone development in the Apert syndrome FGFR2(+/S252W) mouse. Development 2005;132:3537–48. [PubMed: 15975938]

Warren SM, Brunet LJ, Harland RM, Economides AN, Longaker MT. The BMP antagonist noggin regulates cranial suture fusion. Nature 2003;422:625–9. [PubMed: 12687003]

Wilkie AO, Slaney SF, Oldridge M, Poole MD, Ashworth GJ, Hockley AD, Hayward RD, David DJ, Pulleyn LJ, Rutland P, et al. Apert syndrome results from localized mutations of FGFR2 and is allelic with Crouzon syndrome. Nat Genet 1995;9:165–72. [PubMed: 7719344]

Xu, Q.; Wilkinson, DG. In situ hybridization of mRNA with hapten labelled probes. In: Wilkinson, DG., editor. In Situ Hybridization: A Practical Approach. Oxford University Press; Oxford: 1999. p. 87-106.

Yang F, Wang Y, Zhang Z, Hsu B, Jabs EW, Elisseeff JH. The study of abnormal bone development in the Apert syndrome Fgfr2+/S252W mouse using a 3D hydrogel culture model. Bone 2008;43:55–63. [PubMed: 18407821]

Yoshida T, Vivatbutsiri P, Morriss-Kay G, Saga Y, Iseki S. Cell lineage in mammalian craniofacial mesenchyme. Mech Dev 2008;125:797–808. [PubMed: 18617001]

Yu K, Herr AB, Waksman G, Ornitz DM. Loss of fibroblast growth factor receptor 2 ligand-binding specificity in Apert syndrome. Proc Natl Acad Sci USA 2000;97:14536–41. [PubMed: 11121055]

Yu K, Xu J, Liu Z, Sosic D, Shao J, Olson EN, Towler DA, Ornitz DM. Conditional inactivation of FGF receptor 2 reveals an essential role for FGF signaling in the regulation of osteoblast function and bone growth. Development 2003;130:3063–74. [PubMed: 12756187]

Zhou YX, Xu X, Chen L, Li C, Brodie SG, Deng CX. A Pro250Arg substitution in mouse Fgfr1 causes increased expression of Cbfa1 and premature fusion of calvarial sutures. Hum Mol Genet 2000;9:2001–8. [PubMed: 10942429]

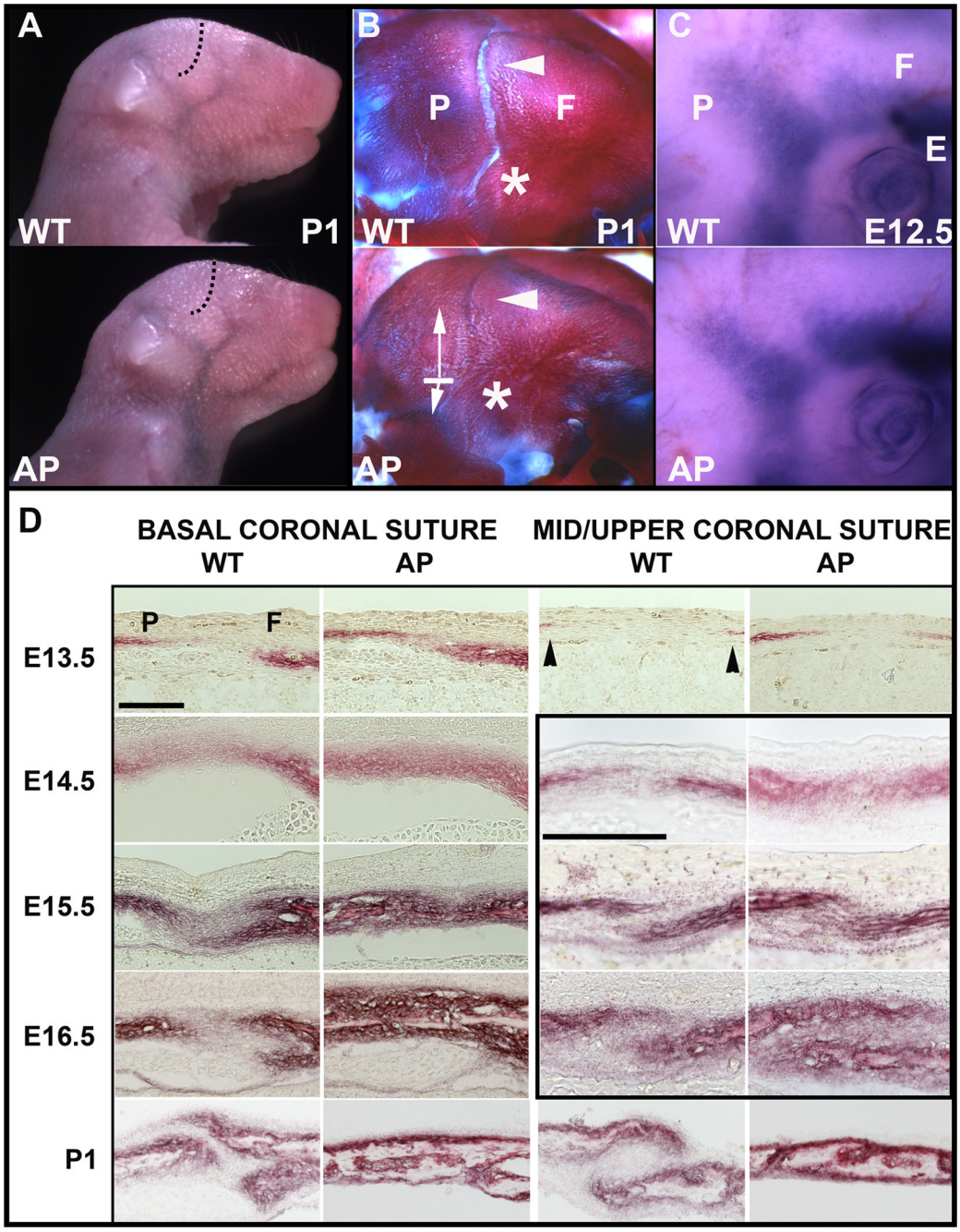

Fig. 1.

Coronal synostosis in the *Fgfr2*$^{S252W/+}$ calvaria. (A) Newborn (P1) *Fgfr2*$^{S252W/+}$ (AP) pups have domed heads and short faces compared to wild-type (WT) littermates. Dotted line, approximate position of coronal suture. (B) Alizarin red/alcian blue staining of newborn skulls shows synostosis of the basal (asterisk) and mid/upper (arrowhead) *Fgfr2*$^{S252W/+}$ coronal suture. The long and short arrows extending from the horizontal bar indicate the major and minor directions of fusion from the starting point, discussed later. (C) Staining of whole calvaria for Alp activity in osteogenic domains of the frontal (F) and parietal (P) anlagen shows no clear differences between WT and AP littermates at E12.5 (E, eye). (D) Staining for Alp activity in transverse sections of the coronal suture of WT and AP calvaria between E13.5 and

P1. The osteogenic fronts rapidly coalesce in the basal *Fgfr2*$^{S252W/+}$ suture. In the mid/upper *Fgfr2*$^{S252W/+}$ coronal suture a relatively normal suture morphology is initially established by E15.5, but is slowly eliminated as OFs fuse. The endocranial surface is at the lower side of each panel. Vertical arrowheads at E13.5, frontal and parietal edges. Scale bars, 100 μm, apply to boxed areas.

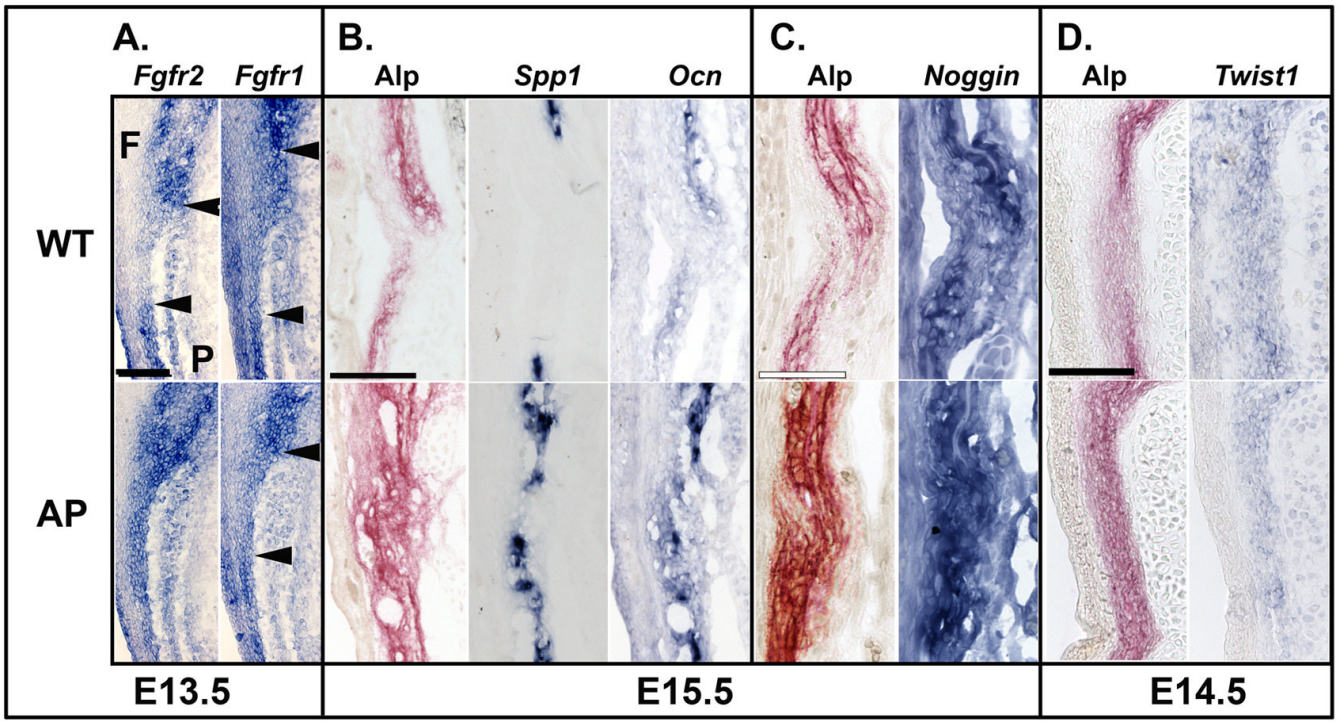

Fig. 2.

Osteoblast gene expression in the *Fgfr2*$^{S252W/+}$ coronal suture (RNA ISH). (A) At E13.5, the frontal and parietal domains of *Fgfr2* and *Fgfr1* expression are distinct in the WT suture, but in the basal *Fgfr2*$^{S252W/+}$ suture *Fgfr2* expression starts to become continuous between the frontal and parietal domains, while *Fgfr1* domains are closer. (B) *Spp1* and *Ocn* are more widely expressed compared to the WT in fusing *Fgfr2*$^{S252W/+}$ sutures. (C) *Noggin* is not down-regulated in fusing *Fgfr2*$^{S252W/+}$ sutures. (D) Only mild changes in *Twist1* expression are seen in fusing sutures. Transverse sections are adjacent (A, D) or near-adjacent (B, C), with the endocranial surface to the right. Black bars, 100 μm; white bar, 50 μm.

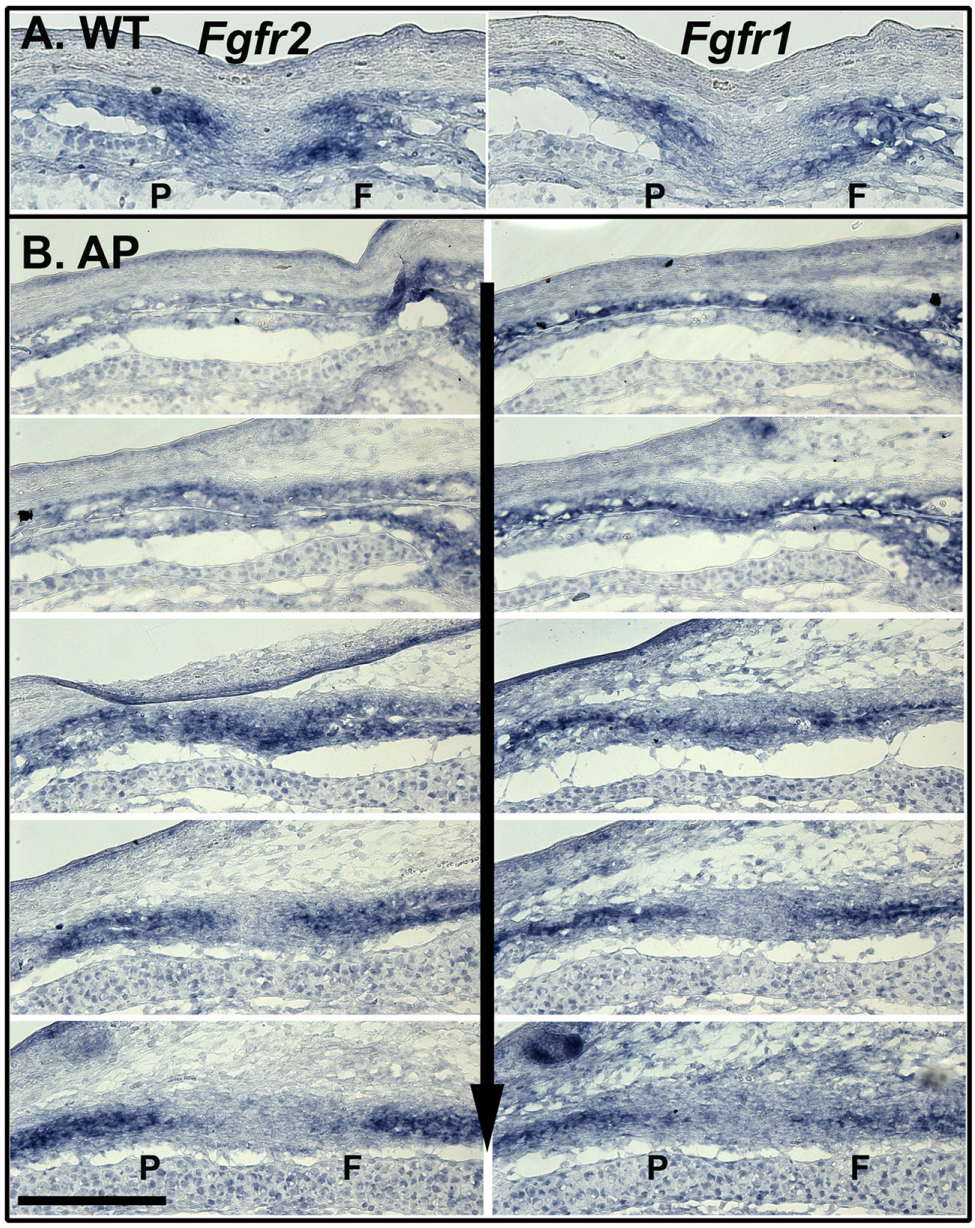

Fig. 3.

Obliteration of the basal coronal suture. ISH for *Fgfr2* (left column) and *Fgfr1* (right column) in transverse sections of E15.5 WT (3A) and *Fgfr2*$^{S252W/+}$ (AP, 3B) calvaria. In 3B, the spatial progress of the OFs during fusion in a single coronal suture is shown in serial sections, proceeding from a point of fusion in the highest panel (equivalent to the position of the WT sections in 3A) towards the base of the suture in the lowest panel (direction of vertical arrow; see small arrow in Fig. 1B). Serial sections are separated by 90 μm in the vertical direction. P, parietal; F, frontal. The endocranial surface is at the lower side of each panel. Bar, 100 μm.

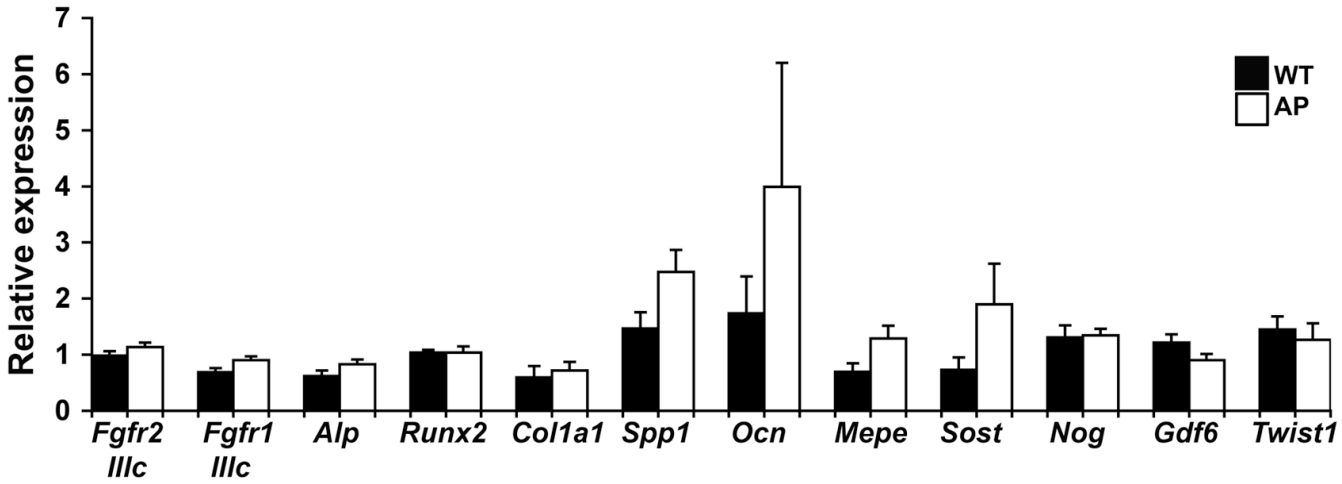

Fig. 4.

Osteoblast gene expression in E15.5 calvaria. Quantitative real-time RTPCR of RNA from WT (black; WT) and *Fgfr2*$^{S252W/+}$ (white; AP) whole calvaria shows only minor increases in later differentiation markers in *Fgfr2*$^{S252W/+}$ mice compared to WT levels. Expression levels are shown as the mean ± SEM of three or six WT and three *Fgfr2*$^{S252W/+}$ samples, relative to a single WT sample for each gene. Differences in expression levels between WT and *Fgfr2*$^{S252W/+}$ samples were not significant when analyzed by the Student's *t* test.

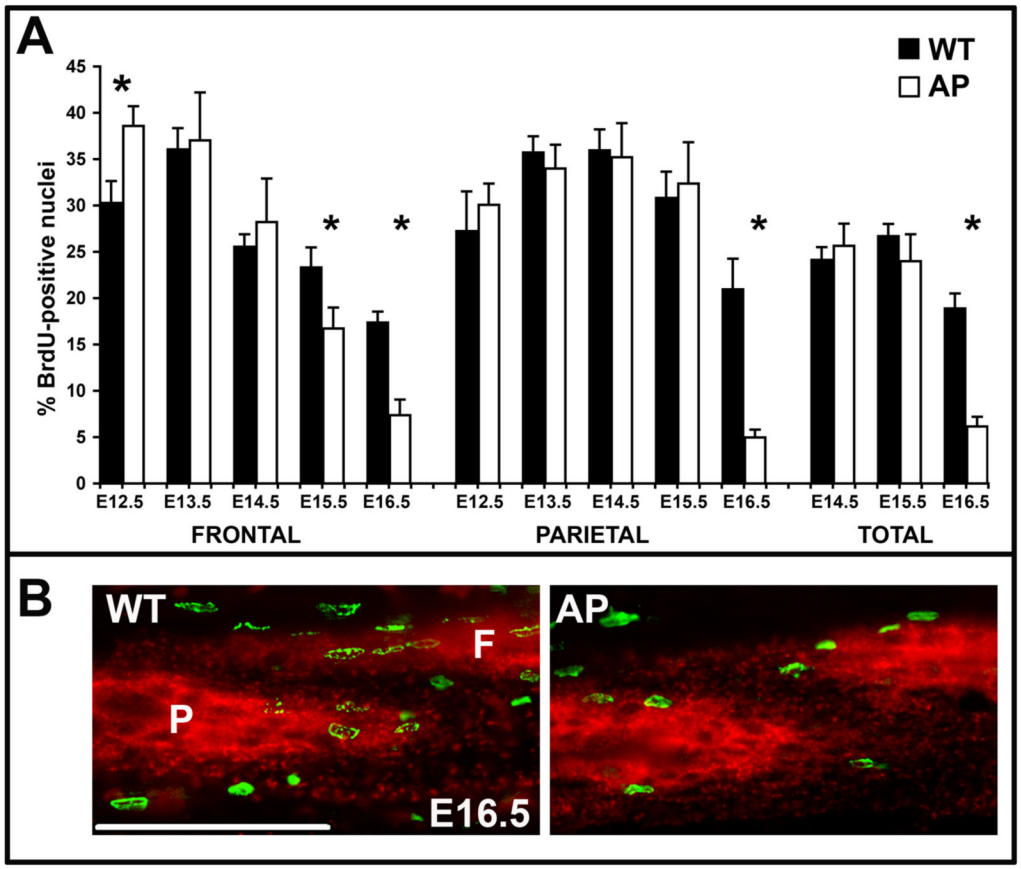

Fig. 5.

Proliferation in coronal sutures during embryonic calvarial development. (A) The number of BrdU-positive nuclei is shown as a percentage of total nuclei within defined regions of the individual OFs (frontal and parietal) or total (frontal plus parietal) sutures between E12.5 and E16.5. WT, black; AP (*Fgfr2*$^{S252W/+}$), white. Values are shown as the mean ± SEM of 4–7 alternate sections of a single suture. Asterisks indicate statistically significant differences determined using the Student's *t* test (Frontal: E12.5, P= 0.039; E15.5, P= 0.040; E16.5, P= 0.003; Parietal: E16.5, P= 0.004; Total: E16.5, P= 0.0004). (B) At E16.5, proliferation (BrdU incorporation, green nuclei) within OFs (Alp-expressing domains, red) is decreased in upper *Fgfr2*$^{S252W/+}$ sutures in advance of suture fusion. Bar, 70 μm.

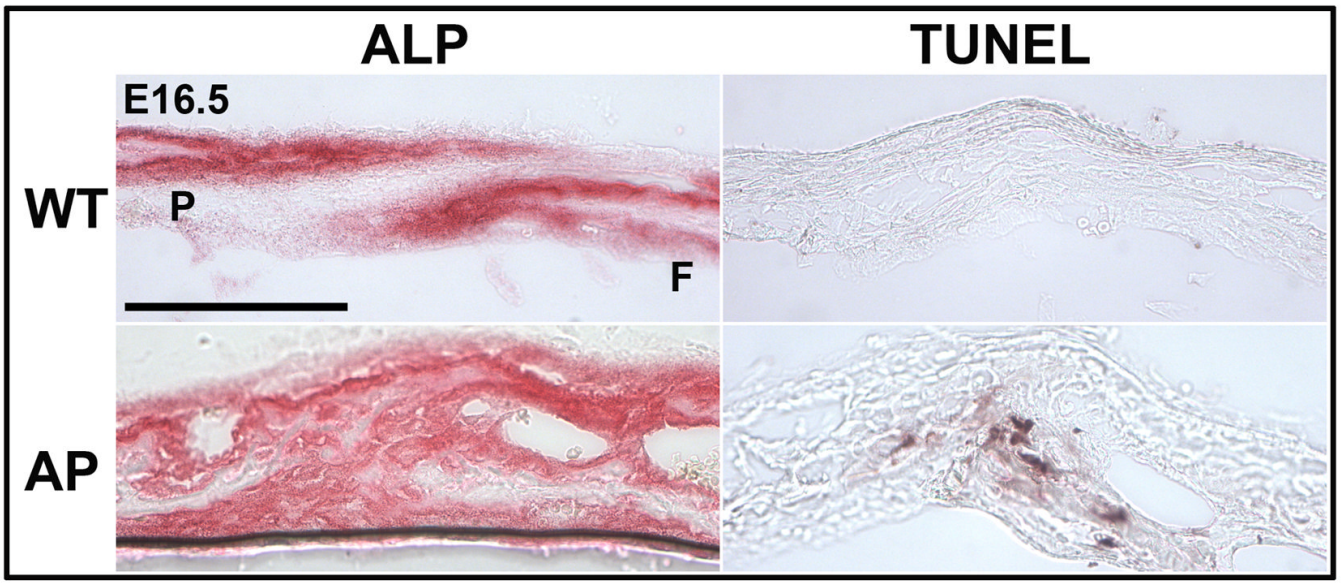

Fig. 6.

Apoptosis during coronal suture fusion. TUNEL-positive cells were only seen in later *Fgfr2*$^{S252W/+}$ coronal sutures (E16.5) in areas of frontal and parietal osteoid contact. WT, wild type; AP, *Fgfr2*$^{S252W/+}$; ALP, alkaline phosphatase. Bar, 100 μm.

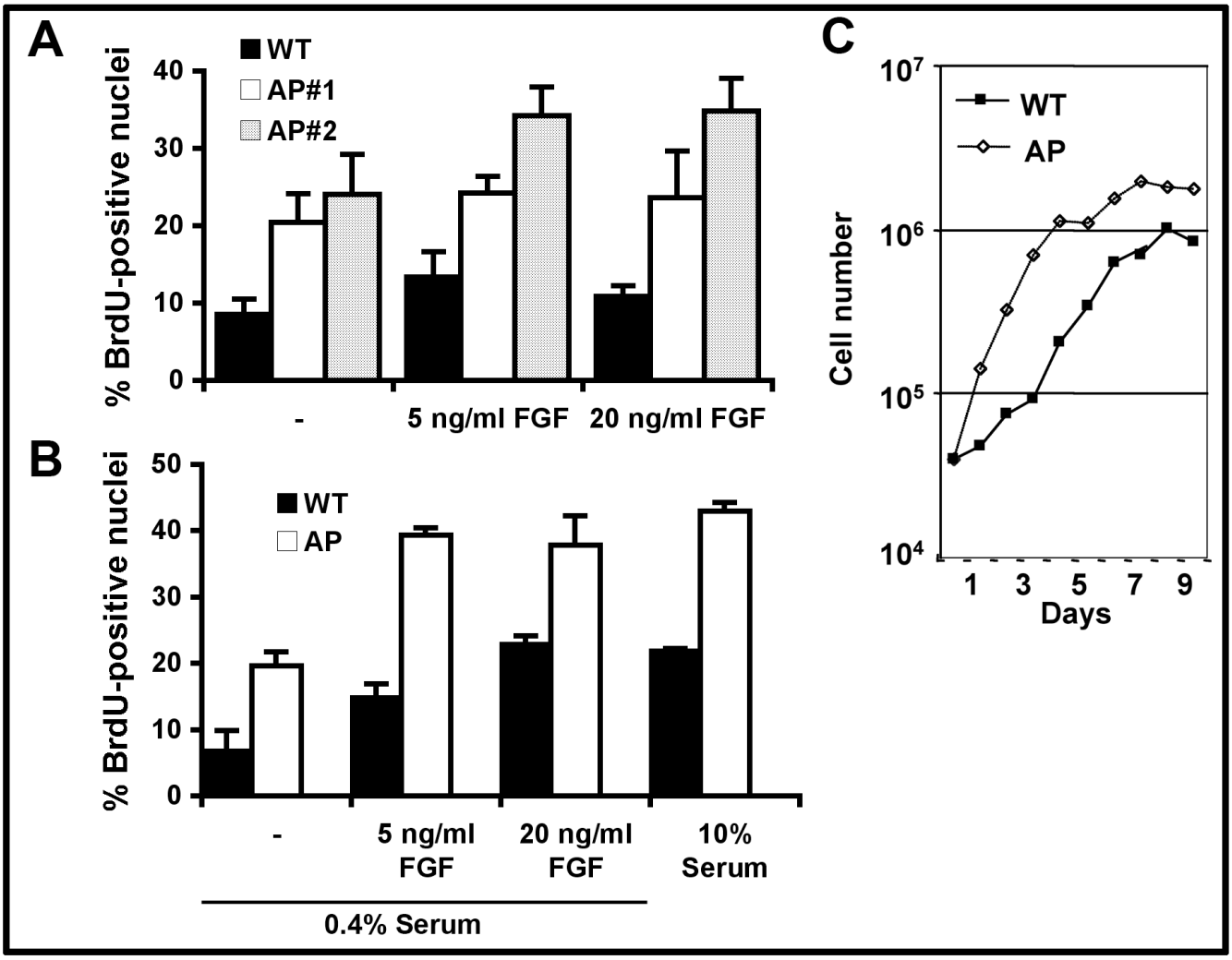

Fig. 7.

Proliferation of WT and *Fgfr2*$^{S252W/+}$ osteoblasts in culture. (A, B) BrdU incorporation into primary (A) and immortalized (B) *Fgfr2*$^{S252W/+}$ (white, grey) and WT (black) cells. Cells were grown in either 10% (A) or 0.4% (B) serum, then treated with FGF1 for 24 hours, with BrdU added for the last 4 hours. (C) Growth curve of *Fgfr2*$^{S252W/+}$ (open diamonds) and WT (black squares) osteoblasts. Cells were grown in 10% FCS.

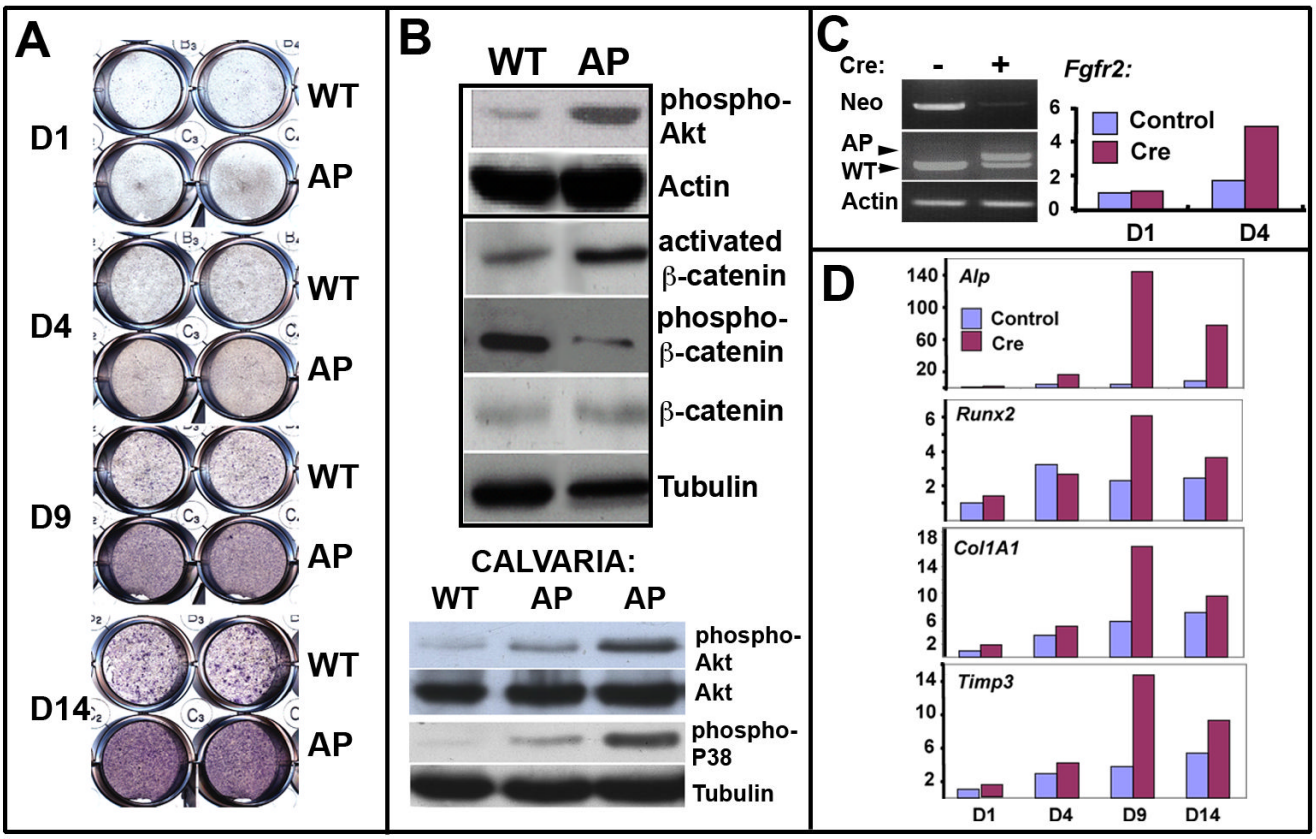

Fig. 8.

Differentiation of *Fgfr2*$^{S252W/+}$ and WT osteoblasts in culture. (A) Time course of Alp activity of immortalized *Fgfr2*$^{S252W/+}$ (AP) and WT cells in differentiation medium. (B) Western blots showing greater activation of signaling proteins involved in differentiation in immortalized *Fgfr2*$^{S252W/+}$ (AP) compared to WT osteoblasts (upper panel) and in newborn calvaria (lower panel). (C) Induction of *Fgfr2*^{S252W} expression by *Cre* virus infection of immortalized *Fgfr2*$^{NeoS252W/+}$ osteoblasts, compared to control infection, shown by gDNA PCR (left) and quantitative real-time RTPCR (right). (D) The control- and *Cre*-infected cells in (C) were incubated in differentiation medium, and the relative expression levels of various osteoblast differentiation markers were determined by quantitative real-time RTPCR on the days indicated.